

# Systematic of Alcohol-Induced Simple Coacervation in Aqueous Gelatin Solutions

B. Mohanty and H. B. Bohidar\*

School of Physical Sciences, Jawaharlal Nehru University, New Delhi 110016, India

Received March 17, 2003

Turbidity measurements performed at 450 nm were used to follow the process of simple coacervation when 1% (w/v) aqueous alkali processed gelatin (type-B) solutions were titrated with methanol, ethanol, propanol, and *tert*-butyl alcohol at various pHs of the solution ranging from pH = 5 to 8 and ionic strengths varying from  $I = 0.01$  to 0.1 M NaCl. The titration profiles clearly established the transition points in terms of the percentage of volume of alcohol added relative to that of solvent corresponding to the first occurrence of turbidity ( $V_t$ ) and a point of turbidity maximum ( $V_p$ ). Addition of more alcohol drove the system toward precipitation. The values of  $V_t$  and  $V_p$  characterized the initiation of intramolecular folding and intermolecular aggregate formation of the charge neutralized gelatin molecules and the subsequent micro coacervate droplet formation. The state of intermolecular aggregates and that of folded gelatin molecules could be characterized by dynamic laser light scattering experiments, which implied spontaneous segregation of particle sizes preceding coacervation. The aggregates constitute the coacervate phase while the folded gelatin molecules mostly stay dispersed in the supernatant. The data taken together reveal the role played by solution entropy in addition to that of electrostatic and solute–solvent interactions, which had been overlooked hitherto.

## I. Introduction

Coacervation has been studied most extensively in aqueous solutions of charged synthetic or biological macromolecules in the last couple of decades.<sup>1–5</sup> The details of this process has been described in the pioneering work of Bungenberg de Jong.<sup>6</sup> The features associated with coacervation have been summarized in detail in several references.<sup>7–9</sup> Potential applications of coacervates are many starting from protein purification<sup>10</sup> and drug encapsulation<sup>11</sup> to treatment of organic plumes,<sup>12</sup> etc. This calls for better understanding of the coacervate structure and transport of macromolecules inside this phase.<sup>1</sup> Realizing that this has direct bearing on transport of proteins through membranes, the importance of these studies can be hardly stressed.

Coacervation is a process during which a homogeneous solution of charged macromolecules, undergoes liquid–liquid phase separation, giving rise to a polymer rich dense phase. Coacervation has been classified into simple and complex processes depending on the number of participating macromolecules.<sup>6</sup> In simple polyelectrolyte coacervation, addition of salt or alcohol normally promotes coacervation.<sup>6</sup> In complex coacervation, two oppositely charged macromolecules (or a polyelectrolyte and an oppositely charged colloid) can undergo coacervation through associative interactions.<sup>13</sup> The charges on the polyelectrolytes must be sufficiently large to cause significant electrostatic interactions but not so large to cause precipitation. The dilute liquid phase, usually the supernatant, remains in equilibrium with the coacervate phase. These two liquid phases are incompat-

ible and immiscible. The protein–polyelectrolyte system is a special case of colloid–polyelectrolyte coacervates. In these systems, interactions primarily arising from electrostatic forces lead to coacervation. Protein–polyelectrolyte coacervates are a novel state of matter, where the concentration of bound protein can reach a level of  $\approx 150$  g/L normally unsustainable in aqueous solutions.<sup>6</sup> It must be noted here that coacervation is not same as precipitation. Coacervates are polymer-rich super concentrated solutions that remain in equilibrium with the supernatant. The investigation of basic aspects of coacervation of polyelectrolyte complexes provides a foundation not only for the basic understanding of these supramolecular structures but also for their practical applications to protein-related industrial process.

In a recent work,<sup>14</sup> turbidity and light scattering measurements along with phase contrast microscopy were used to follow the processes leading to coacervation when aqueous solutions of bovine serum albumin (BSA) and poly(dimethyldiallylammonium chloride) (PDADMAC) were brought from pH = 4 to 10. The state of macromolecular assembly of complexes formed between BSA and PDADMAC prior to and during the pH-induced coacervation could be characterized by specific pH values at which recognizable transitions took place. Based on the pH-induced evolution of scattering intensity measurements, it was concluded that the formation of soluble primary protein–polymer complexes is initiated at  $pH_c$  and this proceeds until  $pH_\phi$ . A maximum in scattering intensity at  $pH_\phi$  is observed coincident with the appearance of turbidity and also corresponding to the first microscopic observation of coacervate droplets. The tem-

\* To whom correspondence should be addressed. E-mail: bohi0700@mail.jnu.ac.in.

perature and protein to polymer concentration ratio dependence of  $pH_c$  and  $pH_\phi$  were studied explicitly.

A survey of literature confirms the near total absence of systematic studies on simple coacervate systems. Gelatin, a polyampholyte obtained from denatured collagen, is a polypeptide and is an ideal case for such studies. The chemical composition of this biopolymer is as follows (as per Merck index): Glycine constitutes 26%; alanine and arginine are in 1:1 ratio together and constitute  $\approx 20\%$ ; proline is  $\approx 14\%$ ; glutamic acid and hydroxyproline are in 1:1 ratio and constitute  $\approx 22\%$ ; aspartic acid  $\approx 6\%$ ; lysine  $\approx 5\%$ ; valine, leucine, and serine constitute  $\approx 2.0\%$  each; the rest, 1%, is comprised of isoleucine and threonine, etc. The aqueous solution properties of gelatin have been well studied and characterized in the past.<sup>15,16</sup> Depending on the process of recovery, the gelatin molecules bear different physical characteristics. Type-A gelatin is acid processed and has an isoelectric pH,  $pI \approx 9$ , whereas the alkali processed type-B gelatin has  $pI \approx 5$ .<sup>17</sup> In the past, all of the coacervation studies on gelatin involved complexation between type-A and type-B or gelatin and acacia molecules.<sup>18–22</sup>

The experimental data obtained from such studies were used to test the theoretical models proposed by (i) Overbeek–Voorn,<sup>23</sup> (ii) Veis–Aranyi,<sup>20,24</sup> (iii) Nakajima–Sato,<sup>25</sup> and (iv) Tainaka.<sup>26</sup> The Overbeek–Voorn model estimates the total free energy of the system as a sum of electrostatic free energy (between pairs of charged sites of gelatin molecules) and free energy of mixing estimated on the basis of Flory–Huggins solute–solvent interaction. This model downplays the role of solute–solvent interactions and yields a coacervation condition given by  $\sigma^3 r \geq 0.53$  for two component systems. Here  $\sigma$  is the charge density of the polyelectrolyte and  $r$  is the number of sites occupied by the gelatin molecule (basically equivalent to molecular weight). Thus, both high molecular weight and large charge density facilitate coacervation. For three component systems (in the presence of micro-ions),  $\sigma^3 r \geq 1.06$ .

Veis–Aranyi<sup>20</sup> proposed a model for coacervation between type-A and type-B gelatin molecules, popularly referred to as the *dilute phase aggregation model* which undermines the electrostatic interactions and postulates the formation of complex coacervates through solute–solvent interactions characterized by the Flory–Huggins interaction parameter  $\chi$  assuming nonzero heat of mixing. In the Flory–Huggins picture,  $\chi$  has only an enthalpy term in it, whereas Veis–Aranyi argue the presence of an additional configurational entropy term. Correspondingly,  $\chi$  is not proportional to  $1/T$ , where  $T$  is the solution temperature. The proportionality is valid only in the absence of entropic contribution to  $\chi$ . In this model, the heat of mixing,  $\Delta H_m$ , is proportional to  $\chi$  and one observes coacervation even when  $\sigma^3 r \leq 0.53$  contrary to the Overbeek–Voorn prediction.

In the Nakajima–Sato model,<sup>25</sup> the Overbeek–Voorn treatment was formalized by inclusion of the solute–solvent interactions in the calculations through Flory–Huggins prescriptions. This model was applied to the data obtained from coacervation of nearly symmetrical poly(vinyl alcohol) molecules of high charge density.<sup>25</sup> Regardless, the model rests on the Overbeek–Voorn presumption that the poly-

electrolyte charges are distributed uniformly both in the dilute and concentrated phase. In the Tainaka model,<sup>26</sup> complementary charge pairing between polyelectrolyte molecules in the dilute phase occurs following the Veis–Aranyi proposition. The main assertion of this model is that the aggregates are symmetrical in charge distribution and size regardless of the same of polyions. Tainaka used the virial coefficient expansion procedure, which Veis<sup>24</sup> applied in the dilute phase, for both phases. This model is not restricted to low charge density polyions, although the Veis–Aranyi critical condition for phase separation had to be met. However, at large charge density, the polyion becomes too stiff to form charge-neutralized complexes. All these models agree on the suppression of coacervation at high ionic strength. Unfortunately, none of these models adequately explain the underlying dynamics of liquid–liquid phase separation preceding complex coacervation. Burgess,<sup>27</sup> through a series of experiments performed on gelatin-acacia and alginic acid-albumin systems, has shown the relative merits of various models.

In the present work, we have undertaken a qualitative and yet a systematic study on simple coacervation of type-B gelatin (a low charge density molecule<sup>26</sup>) in aqueous environment under various thermodynamic conditions of the solvent with a long-term objective to understand the kinetics of simple coacervation. No such study has ever been undertaken despite the fact that such an understanding may serve as a precursor to the mapping of the complexities of coacervation phenomena.

## II. Materials and Methods

All of the alcohols used (i.e., methanol, propanol, and *tert*-butyl alcohol) were obtained from Sisco Laboratories India. Ethanol was obtained from Merck, Germany. Gelatin (type-B, microbiology grade devoid of *E. coli* and liquifier presence) and sodium chloride were bought from E. Merck, India. We used gelatin samples of both type-A (porcine skin extract, bloom = 175 and 300) and type-B (bovine skin extract, bloom = 75) for bloom strength dependence studies, obtained from Sigma Chemicals (USA). The molecular weights of all these samples were estimated from SDS/PAGE and were found to be  $(90 \pm 10)$  kDa. All other chemicals used were bought from Thomas Baker, India. All of the chemicals were of analytical grade. The gelatin samples were used as supplied. The iso-electric pH ( $pI$ ) of gelatin stock solution (1% w/v aqueous solution) was measured with pH titration where we added 0.1 M HCl and 0.1 M NaOH to vary the solution pH, and interestingly, the turbidity data (i.e. 100%  $T$ , where  $T$  is transmittance in percent) data showed a clear peak corresponding to  $pH \approx 5$  which is the nominal  $pI$  of the gelatin used (see Figure 1).

The solvent used was deionized water, and the pH (using 0.1 M HCl or 0.1 M NaOH) and ionic strength of the solvent were first set as per the experimental requirement and the gelatin solutions (1% w/v) were prepared by dispersing gelatin in this medium at 60 °C. The macromolecules were allowed to hydrate completely; this took 30 min to 1 h. The gelation concentration of gelatin in water is  $\approx 2\%$  (w/v), the

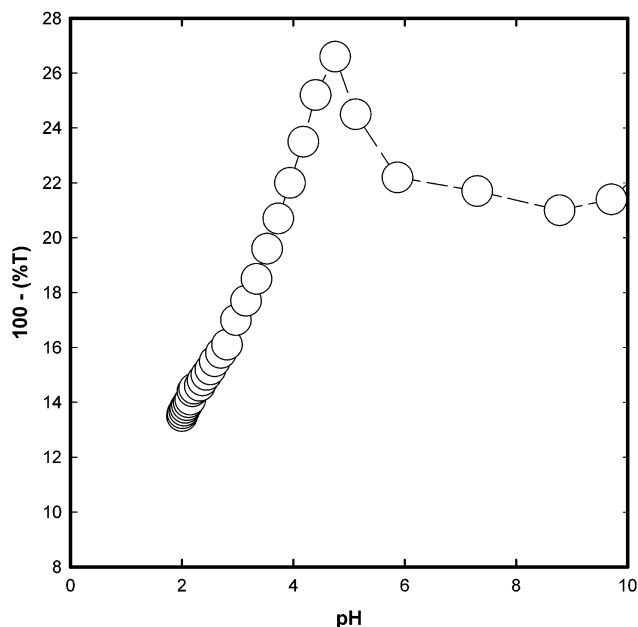


**Figure 1.** Confirmation of iso-electric point from the variation of pH versus turbidity (100%  $T$ ,  $T$  is transmittance) data for a 1% (w/v), 0.1M aqueous gelatin (type-B) solution.

gelatin concentration chosen in these experiments was deliberately kept lower than this to avoid formation of gels.<sup>16</sup>

The particle sizing measurements were done by dynamic laser light scattering (DLS) technique, using a Brookhaven-9000AT digital auto-correlator (Brookhaven Instruments, USA) and a homemade goniometer. The excitation source was a diode pumped solid-state laser (model DPY 305-II, Adlas, Germany) emitting 50 mW of power at 532 nm in linearly polarized single frequency mode. The scattering angle was fixed at 90° and the data analysis was done using CONTIN software provided by Brookhaven Instruments. More on DLS and data analysis can be found elsewhere.<sup>28</sup> We performed SDS/PAGE on all of the samples systematically at various titration stages to ensure the absence of degradation of gelatin.

**Turbidimetric Titration.** Typically, 100 mL of stock solution (1% w/v aqueous gelatin) was taken in a beaker kept on a magnetic stirrer and was stirred at moderate speed with stir bars throughout the titration process. The change in transmittance of the solution was monitored continuously using a turbidity meter (Brinkmann-910, Brinkmann Instruments, USA) operating at 450 nm. Alcohol was taken in a calibrated buret and added in drops to the reaction beaker, and the volume of alcohol added to produce the first occurrence of turbidity was measured ( $V_t$ ), and the process was continued until a turbidity maximum was noticed ( $V_p$ ). Addition of more alcohol drove the system toward precipitation point. The values of  $V_t$  and  $V_p$  characterized the initiation of intramolecular folding and intermolecular aggregate formation of the charge neutralized gelatin molecules. The typical persistence length<sup>15,16</sup> of gelatin in 2 nm imparts enough flexibility to the positively charged segments to overlap (both inter and intra) on negatively charged segments through electrostatic interactions thus neutralizing charges of the segments involved, and the subsequent micro coacervate droplet formation. It must be realized that the gelatin

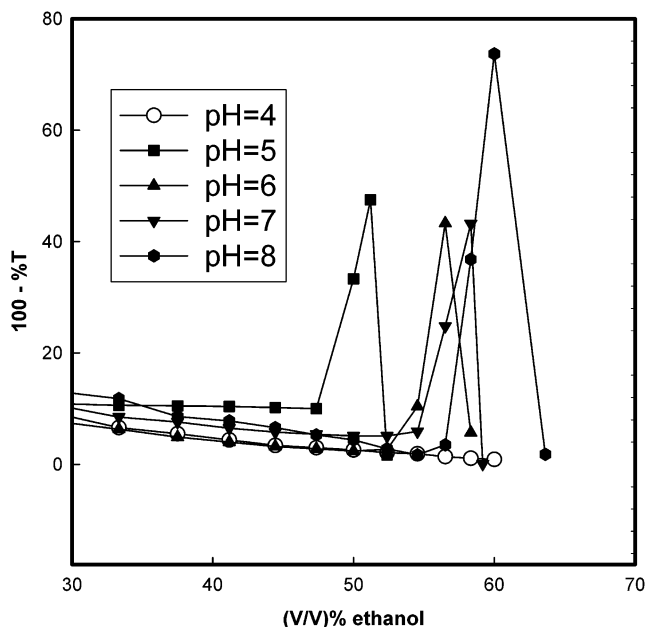


**Figure 2.** Effect of pH on the turbidity of the solution. Titration data for ethanol/water system for a 1% (w/v) aqueous gelatin (type-B) solution with  $I = 0.1$  M performed at 25 °C. Notice the absence of  $V_t$  and  $V_p$  for solutions having pH = 4, which is less than  $pI$  of gelatin.

molecules do carry positive and negatively charged segments at all pHs, though at some pHs there is excess of one type. This, however, does not change the overall picture of coacervation. It will only affect the degree of charge neutralization in a coacervates solution.

The experimental procedure was repeated at different temperatures using a thermostatic water bath providing a temperature stability of  $\pm 1$  °C in the temperature range 35–55 °C. The pH of the reaction mixture was monitored continuously during this process. A typical titration curve is shown in Figure 2. The general observation has been that as one proceeds from methanol to *tert*-butyl alcohol both  $V_t$  and  $V_p$  values decrease. With higher alcohols (beyond *tert*-butyl alcohol), a serious miscibility problem with the solvent was observed at room temperature, thus restricting studies to the first four primary alcohols only. As one moves from methanol to *tert*-butyl alcohol, the hydrophobicity increases. It appears that higher hydrophobicity facilitates formation of charge neutralized aggregates of gelatin molecules that drive the system toward coacervation.

### III. Results and Discussions

#### Phenomenology of the Alcohol-Induced Coacervation

**Process. III.1. Effect of pH.** Figure 2 shows a typical example of the pH dependence of turbidity in the sample solution containing 1% (w/v) gelatin type-B in  $I = 0.1$  M NaCl for a fixed temperature (25 °C) and molecular weight of the polyion. The coacervation process as a function of increasing pH is described in terms of a set of specific values ( $V_t$  and  $V_p$ ) corresponding to the different regions of phase behavior and is clearly identifiable in this figure. For all of the primary alcohols except *tert*-butyl alcohol used in these studies, no  $V_t$  and  $V_p$  values could be obtained when the solution had a pH < 5, i.e., below the isoelectric point, see Figure 3. There

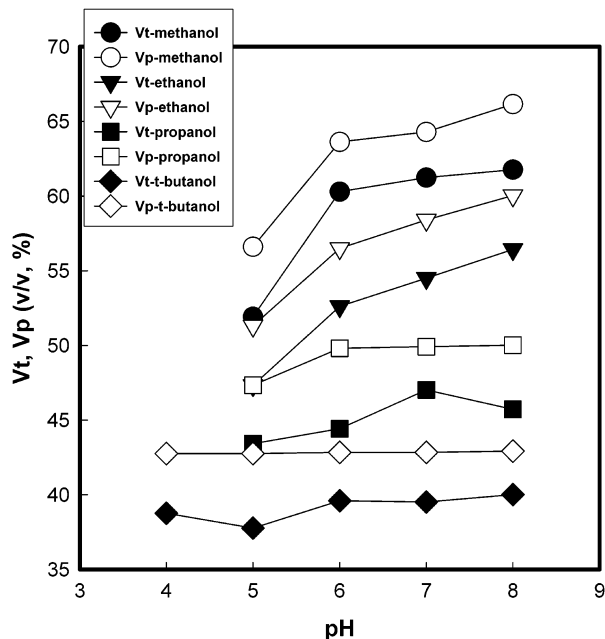


**Figure 3.** Dependence of  $V_t$  and  $V_p$  (both the values are in terms of (v/v)% alcohols/water) on pH for a 1% (w/v) aqueous gelatin (type-B) solution with  $I = 0.1$  M performed at 25 °C. Higher alcohols promote coacervation.

was unusual behavior with respect to the *tert*-butyl alcohol where both  $V_t$  and  $V_p$  values could be measured below the  $pI$  of the biopolymer, i.e., at pH = 4. This appears to be anomalous. It should be mentioned here that during the titration the pH of the solution remained almost the same. For a given ionic strength and molecular weight, lower alcohols show stronger pH dependence requiring larger volumes of alcohol at higher pH for charge neutralization.

For type-B gelatin, it is reported that the zeta potential varies from 0 at pH  $\approx 5$  to  $-70$  mV at pH  $\approx 8$ , a very significant change.<sup>27</sup> Correspondingly, there will be considerable increase in gelatin charge density, which in turn will impart stiffness to the gelatin chain. As seen from Figure 2, at pH = 5 (corresponding zeta potential  $\approx 0$  mV), the coacervation ensues when the ethanol concentration is 45% (v/v). The same happens at pH = 8 (corresponding zeta potential  $\approx -70$  mV) when the ethanol concentration is 60% (v/v). Because gelatin is a polyampholyte, it is possible to reduce the chain stiffness by facilitating electrostatic interactions between charged segments by reducing the dielectric constant of the medium. The strength of electrostatic interactions between two oppositely charged particles increases as  $\epsilon^{-3/2}$  at a given temperature as per the Debye-Huckel theory.<sup>20</sup> The value for the dielectric constant ( $\epsilon$ ) for a 45% (v/v) ethanol solution is  $\approx 56$  and the same for a 60% (v/v) ethanol solution is  $\approx 48$ .<sup>28</sup> Hence, there is a  $8^{3/2} \approx 23$ -fold increase in the strength of electrostatic interaction at pH = 8 which is required to ensue coacervation. The net result is the collapse of gelatin molecules into single-folded chains and aggregates. This will be dealt with further in the discussions involving particle sizing.

**III.2. Effect of Ionic Strength.** Effect of salt concentration on  $V_t$  and  $V_p$  values are summarized in Figure 4. A typical titration curve for methanol is depicted in Figure 5. This figure exhibits the absence of precipitation point for salt

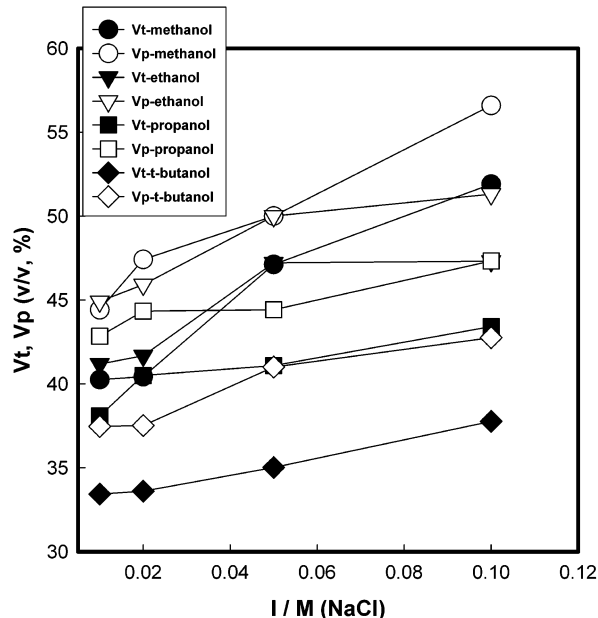


**Figure 4.** Dependence of  $V_t$  and  $V_p$  (both the values are in terms of (v/v)% alcohol/water concentration) on ionic strength  $I$  (in M NaCl), pH = 5 for a 1% (w/v) aqueous gelatin (type-B) solution performed at 25 °C.

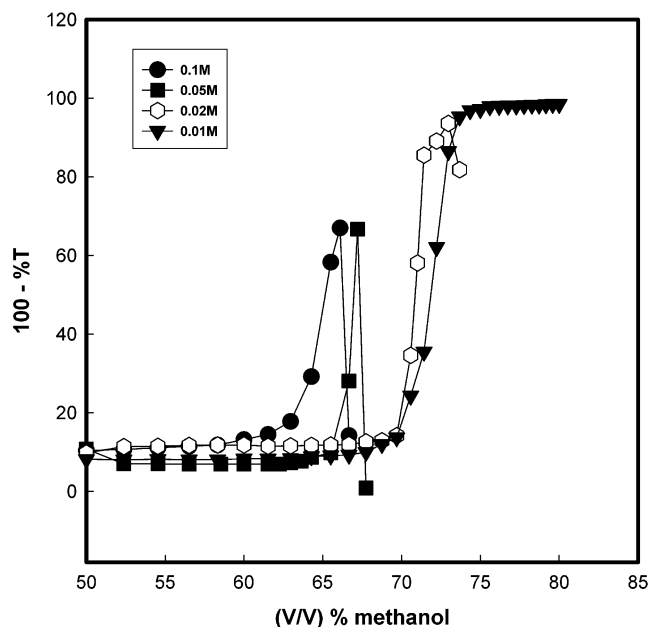


**Figure 5.** Effect of ionic strength,  $I$ , on the turbidity of the solution. Titration profiles shown for methanol/water system for a 1% (w/v) aqueous gelatin (type-B) solution performed at  $T = 25$  °C with pH = 8. Notice the absence of precipitation point for  $I = 0.01$  M data.

concentration  $I < 0.02$  M. The values of  $V_t$  and  $V_p$  were observed to increase with ionic strength at fixed pH, temperature, and molecular weight, and this dependence becomes weaker for higher alcohols (*tert*-butyl alcohol). Beyond the isoelectric pH (i.e., at pH = 7 and pH = 8), it was observed that the  $V_t$  and  $V_p$  values decreased with increase in ionic strength, thus requiring less volume of alcohol for gelatin charge neutralization as shown in Figures 6 and 7. The increase in charge density at pH  $> pI$  would necessitate a higher ionic strength of the solution to enable screening of the electrostatic repulsion between like-charge segments of gelatin molecules. This screening will have two

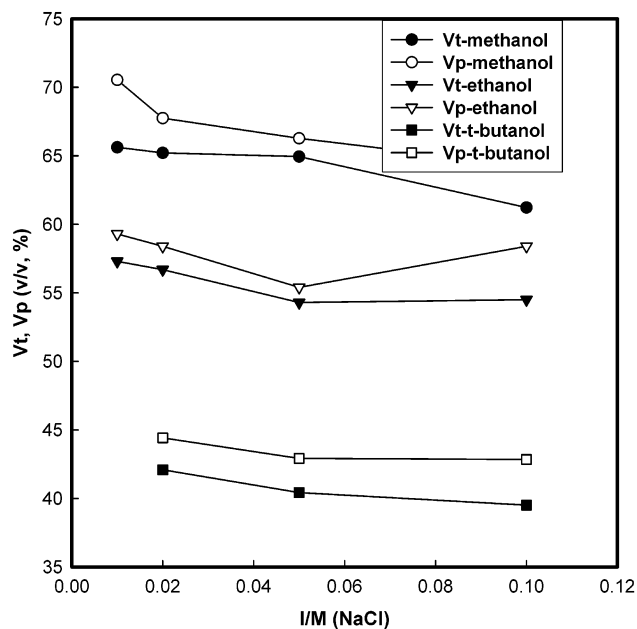


**Figure 6.** Dependence of  $V_t$  and  $V_p$  (both the values are in terms of (v/v)% alcohol/water concentration) on NaCl concentration for a 1% (w/v) aqueous gelatin (type-B) solution with pH = 7 performed at 25 °C.

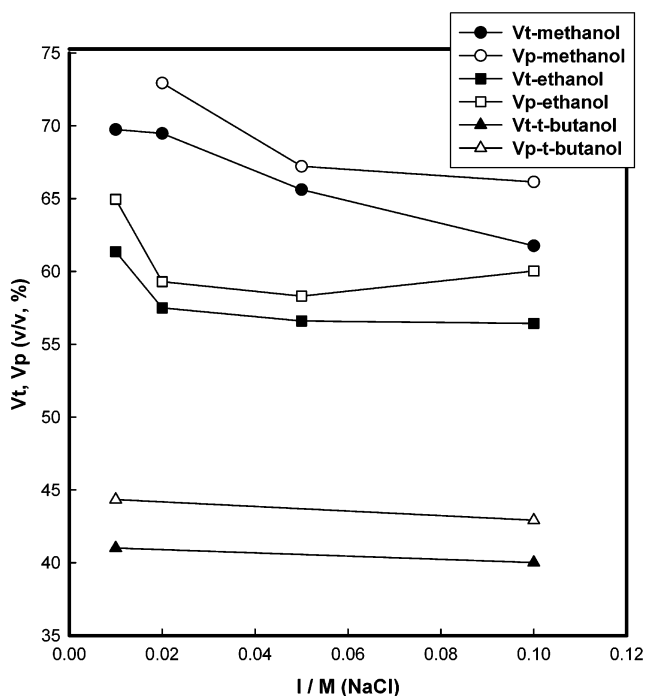


**Figure 7.** Dependence of  $V_t$  and  $V_p$  (both are in terms of (v/v)% alcohol/water) on NaCl concentration for a 1% (w/v) aqueous gelatin (type-B) solution with pH = 8 performed at 25 °C.

consequences: (i) the chain will loose stiffness and (ii) the subsequent folding of single chains or forming intermolecular aggregates can be achieved at much lower  $V_t$  and  $V_p$  values. The experimental data substantiates this. Again it is well-known that higher salt concentration increases hydrophobic interactions. This will imply that higher alcohols (like *tert*-butyl alcohol) will induce coacervation more easily than methanol or ethanol (Figures 6 and 7).

**III.3. Effect of Temperature.** If hydrophobic interaction contribute to coacervation of gelatin molecules, it should be possible to observe the temperature dependence of phase

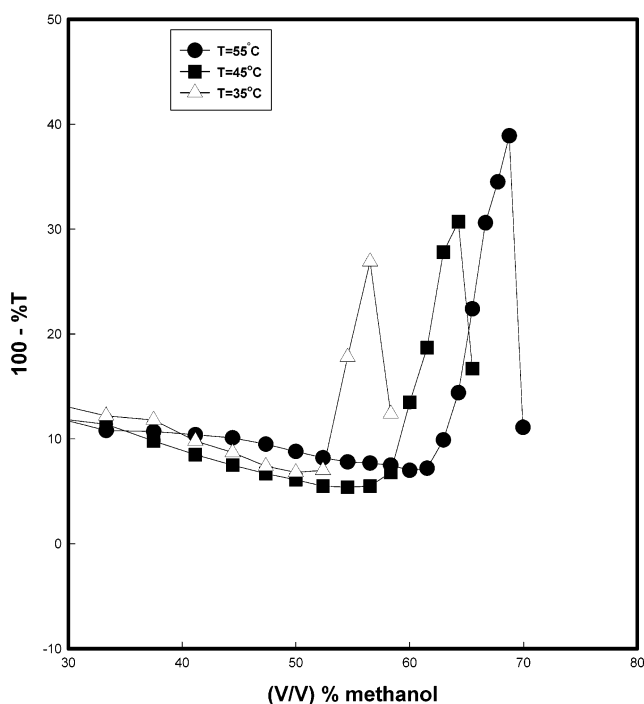


**Figure 8.** Effect of temperature on the turbidity of solutions. Titration profiles are shown for the methanol/water system for a 1% (w/v) aqueous gelatin (Type-B) solution with  $I = 0.1$  M and pH = 5 performed at 25 °C.

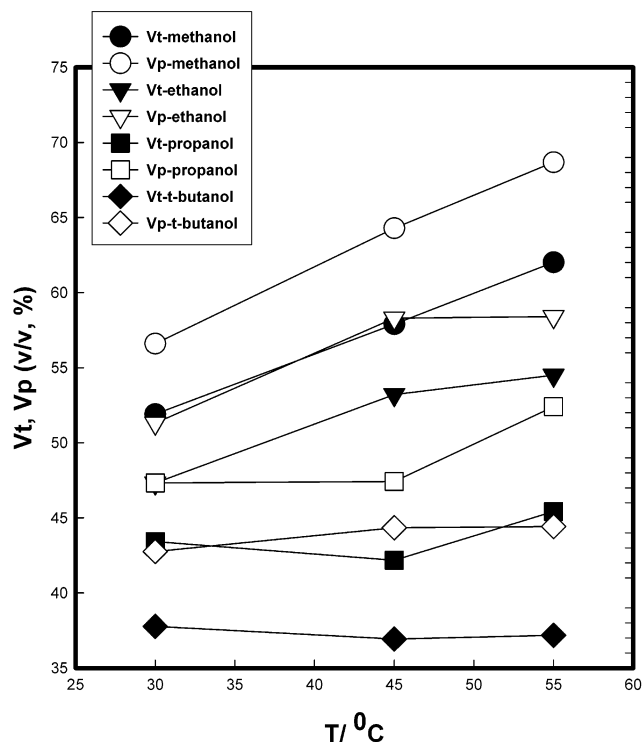


**Figure 9.** Dependence of  $V_t$  and  $V_p$  (both the values are in terms of (v/v)% alcohol/water) on temperatures for a 1% (w/v) aqueous gelatin (type-B) solution with  $I = 0.1$  M performed at pH = 5.

behavior, because hydrophobic interaction are known to exhibit strong temperature dependence. From Figures 8 and 9 it is confirmed that the  $V_t$  and  $V_p$  are shifted to the right with the increase in temperature for fixed ionic strength, pH, and molecular weight ( $I = 0.1$  M, pH = 5). A representative titration feature is shown in Figure 8. Both  $V_t$  and  $V_p$  values exhibit strong temperature dependence for lower alcohols,

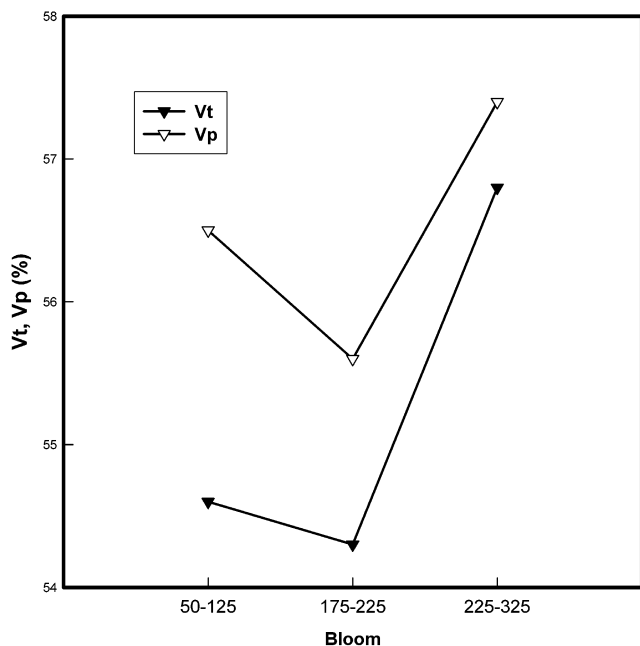


**Figure 10.** Dependence of  $V_t$  and  $V_p$  (in terms of (v/v)% ethanol/water concentration) on molecular weight ( $M$ ) for a 1% (w/v) aqueous gelatin solution with  $I = 0.1$  M and  $\text{pH} = 6$  performed at  $25^\circ\text{C}$ . Lowest molecular weight sample is type-B and others are type-A gelatin samples.

and the effect was observed to be much less for *tert*-butyl alcohol.

The temperature range covered in these studies was limited to  $25\text{--}55^\circ\text{C}$ . Assuming that the initial folding and aggregate formation of gelatin molecules is purely driven by electrostatic effects, one would expect that at higher temperatures the strength<sup>20</sup> of this varying with dielectric constant and temperature as  $(\epsilon T)^{-3/2}$ . A sample calculation with, at  $T = 308$  K corresponding  $\epsilon \approx 79$  and at  $T = 328$  K,  $\epsilon \approx 70$ , yields almost the same value for  $(\epsilon T)^{-3/2} \approx 810 \text{ K}^{-3/2}$ . Thus, the strength of electrostatic interaction between charged segments did not change much in the temperature range of our interest. This raises the question could it be because of hydrophobic effect? This requires further probing.

**III.4. Effect of Bloom Strength.** Bloom strength dependences on  $V_t$  and  $V_p$  are shown in Figure 10 measured at  $I = 0.1$  M,  $\text{pH} = 5$ , and  $T = 30^\circ\text{C}$ . It should be noted here that the lowest bloom sample was type-B gelatin, whereas the other two were type-A samples. The results indicate a very weak dependence of  $V_t$  and  $V_p$  on gelatin bloom strength (less than 5% variation). Since the two types of gelatin molecules have contrasting electrostatic features, these bloom strength dependence studies should be treated as merely qualitative and will not be discussed further.

**III.5. Size of Aggregates.** During the titration process, a few milliliters of the sample was drawn from the reaction beaker and loaded into borosilicate cylindrical cell (volume = 5 mL) and DLS experiment performed. The data analysis revealed two particle sizes all throughout until  $V_p$  was reached. The smaller particles had a size of ca. 20 nm, whereas the aggregates grew in size to reach a value of several hundred nanometers at  $V_p$ . A typical example is shown in Figure 11. For comparison, the value of dielectric constant<sup>29</sup> of the ethanol–water mixture is shown in the same

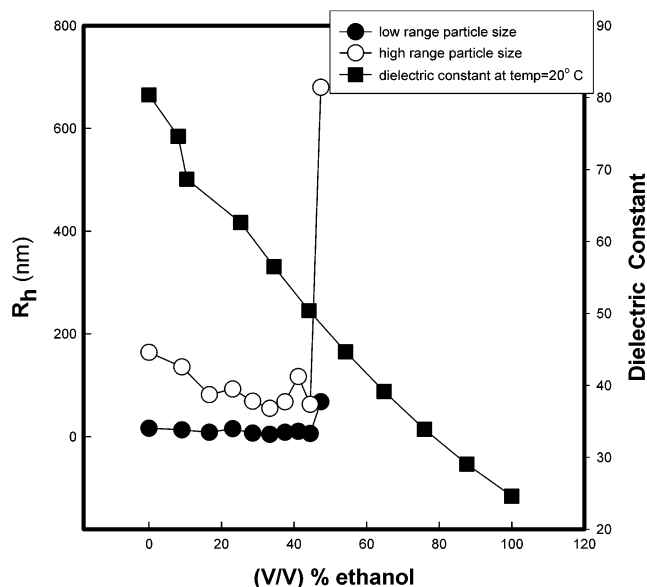


**Figure 11.** Size of various particles measured in terms of hydrodynamic radius ( $R_h$ ) by DLS for a 1% (w/v) aqueous gelatin (type-B) solution titrated with ethanol with  $I = 0.1$  M and  $\text{pH} = 6$  performed at  $20^\circ\text{C}$  (left-hand scale). The dielectric constant ( $\epsilon$ ) data of ethanol/water binary mixture is shown for comparison (right-hand scale).

plot, which shows a monotonic decrease with increased ethanol concentration. Unfortunately for other alcohols and water mixtures, such detailed dielectric constant data is not available in the literature. The results show spontaneous size segregation preceding coacervation, which is consistent with the results reported by Veis.<sup>20,24</sup> Gelatin is not soluble in alcohols, whereas water is a good solvent. As alcohol is added to water, the water molecules will bind with alcohol molecules through hydrogen bonding and the resultant binary mixture becomes a poor solvent for gelatin molecules. Second, the dielectric constant decreases<sup>29</sup> significantly facilitating stronger electrostatic interactions between charged segments (both intra and inter) of gelatin molecules. As has already been mentioned, the strength of electrostatic interactions between two oppositely charged particles increase as  $\epsilon^{-3/2}$  at a given temperature as per the Debye–Huckel theory. The poor solvent quality compels the gelatin molecule to reduce its spatial expansion thereby bringing charged segments to each other's vicinity through electrostatic interactions. This results in the collapse of some of the single gelatin molecules through intramolecular interactions yielding a typical hydrodynamic radius  $\approx 20$  nm, whereas most other molecules associate through intermolecular electrostatic interactions to form large aggregates of radii that are 10 times larger consistent with earlier observations.<sup>19</sup>

#### IV. Conclusion

Addition of alcohol creates a marginal solvent environment for gelatin molecules largely because of the rupture of hydrogen bonds between water molecules and the polyion. This results in the reduction of the overall spatial extension of the polyelectrolyte chain, thereby, bringing the complementary charged segments closer. In a single chain, this leads to self-charge neutralization and formation of gelatin particles of size  $\approx 20$  nm. These are mostly present in the supernatant.

Simultaneously, intermolecular segments of complementary charge form aggregates of size  $\approx 200$  nm. Because these aggregates may not be fully charge neutralized, they can attract other gelatin molecules and thus grow in size. It is shown that the dielectric constant of the medium continuously<sup>29</sup> falls as added alcohol volume increases facilitating stronger electrostatic interactions and, hence, growth in aggregate size. At a critical volume of added alcohol (Vt) the liquid–liquid phase separation ensues. This observation is qualitatively identical to the model proposed by Veis<sup>24</sup> and Tainaka.<sup>26</sup> They argue that the aggregates escape the fate of precipitation because of the configurational entropy gain achieved by randomly mixed heavily concentrated gelatin molecules in the coacervate phase. The solvent in the concentrated phase largely constitutes the solvation liquid. The supernatant is a very dilute polyelectrolyte solution largely containing the gelatin nanoparticles (folded single chains). In Veis model,<sup>24</sup> the aggregates are referred to as symmetrical aggregate polymer (SAP), whereas Tainaka's revised model<sup>26</sup> refers to these as asymmetric aggregate polymer (AAP). Regardless, it is accepted that the coacervate phase owes its origin to these aggregates. Tainaka model<sup>26</sup> assumes Gaussian distribution of segments in AAP aggregates independent of their size and that all of the counterions are bound to the AAP aggregates.

The experimental data presented indicate that the electrostatic interactions between charged segments of this polyion are facilitated by the solute–solvent interactions that turn the solvent from good to marginal enabling a closer approach between charged segments. These segments in turn overlap because of electrostatic interactions. It should be realized that when two oppositely charged segments join together some amount of counterion is always released in to the solvent, there by increasing the entropy of the solution. This will assist the process to move toward coacervation.

The coherent picture that emerges is as follows: (i) that a homogeneous solution containing  $N_1$  molecules of solvent and  $N_2$  molecules of solute at temperature  $T$  and pressure  $P$  will remain stable as long as the free energy of the solute  $F_2$  in solution obeys the thermodynamic condition  $(\partial^2 F_2 / \partial N_2^2)_{N_1, T, O} > 0$ , (ii) that the liquid–liquid phase separation of the coacervate phase from the dilute supernatant is a dehydration (of the individual polyion this is facilitated by the presence of alcohol) process, (iii) that charge neutralization of polyion segments precedes phase separation, and (iv) that the polyions do not precipitate out of the solvent because of entropy gain achieved by random mixing of polyions in

the coacervate phase. In summary, the coacervation proceeds in two steps: first, the selective charge neutralization of polyions dictated by electrostatic interactions and, second, the gain in entropy through random mixing of polyions in the dense phase plus the gain in entropy due to release of counterions to the solvent.

**Acknowledgment.** B.M. is thankful to Council of Scientific and Industrial Research, India for a Junior Research Fellowship. This work was supported by IUC-DAEF research grant (CRS-M-93) and DRS grant of University Grants Commission, India.

## References and Notes

- (1) Smith, A. E.; Bellware, F. T. *Science* **1966**, *152*, 362.
- (2) Smith, A. E. *Science* **1967**, *214*, 1038.
- (3) Oparin, A. P. *The origin of life*; Academic Press: New York, 1957.
- (4) Menger, F. M.; Sykes, B. M. *Langmuir* **1998**, *14*, 4131.
- (5) Tsuchida, E.; Abe, K. *Inter macromolecular Complexes*; Springer: Heidelberg, 1982.
- (6) Bungenberg de Jong, H. G. *In Colloid Science*; Kruyt, H. R., Ed.; Elsevier: New York, 1949; Vol. II.
- (7) *Coulombic interactions in macromolecular systems*; Eisenberg, A., Bailey, F. E., Eds.; American Chemical Society: Washington, DC, 1986; Vol. 302.
- (8) *Ordered Media in Chemical Separation*, Ed.; Hinze, H. L.; Armstrong, D. W., Eds.; American Chemical Society: Washington, DC, 1987; Vol. 342.
- (9) Kokufuta, E. *Prog. Polym. Sci.* **1992**, *17*, 647.
- (10) Dubin, P.; Gao, J.; Mattison, K. *Sep. Purif. Methods* **1994**, *23*, 1.
- (11) Burgess, D. J.; Carless, J. E. *Int. J. Pharm.* **1985**, *27*, 61.
- (12) Wang, Y.; Banziger, J.; Filipelli, G.; Dubin, P. L. *Environ. Sci. Tech.* **2001**, *35*, 2608.
- (13) Park, J. M.; Muhoberac, B. B.; Xia, J. *Macromolecules* **1992**, *25*, 290.
- (14) Kaibara, K.; Okazaki, T.; Bohidar, H.B.; Dubin, P. *Biomacromolecules* **2000**, *1*, 100.
- (15) Bohidar, H. B.; Jena, S. S. *J. Chem. Phys.* **1993**, *98*, 8970.
- (16) Bohidar, H. B.; Jena, S. S. *J. Chem. Phys.* **1994**, *100*, 6888.
- (17) Veis, A. *The macromolecular chemistry of gelatin*; Academic Press: New York, 1964.
- (18) Veis, A.; Cohen, J. J. *Phys. Chem.* **1956**, *78*, 6238.
- (19) Veis, A. *J. Phys. Chem.* **1963**, *65*, 1960.
- (20) Veis, A.; Aranyi, C. J. *Phys. Chem.* **1960**, *64*, 1203.
- (21) Burgess, D. J.; Singh, G. N. *J. Pharm. Pharmacol.* **1993**, *45*, 586.
- (22) Tsung, M.; Burgess, D. J. *J. Pharm. Sci.* **1997**, *86*, 603.
- (23) Overbeek, J.; Voorn, M. J. *J. Cell. Comput. Physiol.* **1957**, *49*, supp-1, 7.
- (24) Veis, A. *J. Phys. Chem.* **1961**, *61*, 1798.
- (25) Nakajima, A.; Sato, H. *Biopolymers* **1972**, *10*, 1345.
- (26) Tainaka, K. *Biopolymers* **1980**, *19*, 1289. Tainaka, K. *J. Phys. Soc. Jpn.* **1979**, *46*, 1899.
- (27) Burgess, D. J. *J. Colloid Interface Sci.* **1990**, *140*, 227.
- (28) Bohidar, H. B. *In Handbook of Polyelectrolytes*; Nalwa, H. S., Ed.; American Scientific Publishers: California, 2002; Vol. II.
- (29) Waller, R.; Strang, T. J. K. *Collection Forum* **1996**, *12*, 70.

BM034080L